



OPEN ACCESS

EDITED BY

Xin Kang,
Hunan University, China

REVIEWED BY

Jue Li,
Chongqing Jiaotong University, China
Yu Liu,
Hunan University, China

*CORRESPONDENCE

Chen Zhang,
✉ 1062715335@qq.com

RECEIVED 25 February 2025

ACCEPTED 15 April 2025

PUBLISHED 14 May 2025

CITATION

Pan C, Zhang C and Ji T (2025) Experimental study of urea-catalyzed microbial solution-based curing of fissured loess soil. *Front. Mater.* 12:1583278. doi: 10.3389/fmats.2025.1583278

COPYRIGHT

© 2025 Pan, Zhang and Ji. This is an open-access article distributed under the terms of the [Creative Commons Attribution License \(CC BY\)](https://creativecommons.org/licenses/by/4.0/). The use, distribution or reproduction in other forums is permitted, provided the original author(s) and the copyright owner(s) are credited and that the original publication in this journal is cited, in accordance with accepted academic practice. No use, distribution or reproduction is permitted which does not comply with these terms.

Experimental study of urea-catalyzed microbial solution-based curing of fissured loess soil

Chaofan Pan¹, Chen Zhang^{1*} and Tuo Ji²

¹Geotechnical Engineering Department, Nanjing Hydraulic Research Institute, Nanjing, Jiangsu, China, ²School of Chemical Engineering, Nanjing Tech University, Nanjing, Jiangsu, China

The ubiquitous vertical cracks in loess areas are one of the main factors that cause disasters in engineering projects, and the restoration of cracked loess is of great significance for disaster prevention. Microbial-induced calcium carbonate precipitation (MICP), as a green solidification method, is widely used in soil remediation. Microstructural changes in crack-free loess after solidification were analyzed using a scanning electron microscope, and the optimal grouting scheme of microbial solution catalyzed by urea was determined. Solidification tests were carried out on fractured loess with different openings, and the solidification effect of MICP was evaluated using the direct shear test. The results show that the surface contact between micro-aggregates and the contact area between soil particles increased greatly after MICP curing. Under the catalysis of urea, the amount of CaCO₃ increased by 30%, which enhanced the strength of the soil on both sides of the fractured loess structural plane after solidification. It provides a solid experimental basis and detailed microscopic explanation for MICP strengthening fractured loess.

KEYWORDS

microbial-induced calcium carbonate precipitation, fissured loess, CaCO₃ production, straight shear test, microanalysis

1 Introduction

Loess is a type of special soil widely distributed in China, which is mainly concentrated in arid and semi-arid areas, and its total coverage area reaches 6.4×10^5 km². Compared with other types of soils, loess has unique engineering characteristics, such as wet subsidence, large soil pores, vertical joints, and other characteristics (Gu and Chen, 2020; Morris and Williams, 2018; Liu H et al., 2022; Yan C G et al., 2023). As one of the key unfavorable factors inducing engineering geohazards, the presence of loess fissures constitutes a significant impact on the stability of its foundation structure. The number, location, inclination, and direction of the fissures are all important parameters affecting the strength properties of fissured loess. Previous studies showed that oblique fissures are more harmful to slope stability than vertical fissures. Fissure joints with the same orientation as the slope have a more prominent effect than those with other orientations (UTILI S 2013; SPENCER E. 1967; Gao Y et al., 2013; Sun P et al., 2016). When the cracked soil body is eroded by rainfall, the soil body on both sides will be softened by water infiltration, leading to misalignment and collapse of the soil body on both sides of the crack. The fissures' development not only exacerbates this destructive process but also triggers



FIGURE 1
Sample of soil sampling from Xianyang city.

further engineering disasters, seriously threatening engineering safety (Li G Y et al., 2018; Zhou J 2019).

Microbial-induced calcium carbonate precipitation (MICP) for soil curing has been favored at home and abroad as an emerging green technology, and it is environmentally friendly and has a controllable reaction process, among other advantages, but its reaction rate is slow (He J et al., 2016). The MICP reaction process first involves the synthesis of bacterial intracellular syntheses and the release of urease, which catalyzes the hydrolysis of urea to generate NH_4^+ and CO_3^{2-} , and then the calcium-containing solution releases calcium ions, finally forming a calcium carbonate precipitate. In order to improve the reaction efficiency of MICP, scholars have studied the urease activity (GUIMARAESGF et al., 2016; Xiao X M et al., 2017), the urea release rate (Jia Y M et al., 2020; Cintia F et al., 2016), the Ca^{2+} release rate, and the CaCO_3 crystallization rate (Luo and Lu, 2000; CLIFFORD Y et al., 2008; He S L et al., 2008), and they have found that urea plays an important role in the process. Therefore, it is significant to clarify the role of urea in the catalytic mechanism of the MICP reaction.

At present, research on MICP technology mostly focuses on the macroscopic mechanical properties of cured, intact soil bodies, while microscopic research mainly focuses on the microscopic morphology before MICP curing (Wei T et al., 2019; Ahmad and Chandra, 2019; Shao X et al., 2018; Jiang M et al., 2014; Li P et al., 2019). Research on the curing of fissured soil bodies and the microscopic analysis of cured soils is still insufficient; particularly, the patterns of microstructural changes in loess after MICP curing by have been rarely studied. The fundamental reason for the change

TABLE 1 Composition of the culture medium and culture solution per 100 ml

Drug name	Liquid nutrient medium	Culture solution
Peptone	0.5 g	---
Beef extract	0.3 g	---
Urea	2 g	---
Yeast extract	---	2 g
NH_4Cl	---	1 g
MnSO_4	---	1 mg
NiCl	---	2.4 mg
Distilled water	100 mL	100 mL

in soil engineering properties lies in its microstructural changes, so the study needs to start from the perspective of macro-micro combination (Muñoz-Castelblanco J. A et al., 2012; Wen and Yan, 2014; Liu Z et al., 2015). At the same time, the precise control of the MICP reaction and the durability of the reaction in the transportation process within the fracture have been less studied, presenting promising prospects for future research (Chen M Y et al., 2023; Chen Y Q et al., 2022; Li et al., 2025).



FIGURE 2
Fracture surface of the specimen.

In this study, the influence of microbial solution on the efficiency of the MICP reaction with or without urea catalysis was investigated. The microbial solution grouting process was optimized by changing the ratio of the bacterial and cementing solutions. The curing test was first conducted on loess specimens without fissures, and the microstructure of the cured loess without fissures was observed using the scanning electron microscope test to reveal the micro-mechanism of MICP-cured loess. A curing test was conducted on the fissured loess, and the effect of fissure width on the curing performance was analyzed using a shear test. It provides a solid experimental foundation and a detailed microscopic explanation for the application of MICP to the reinforcement of fissure loess with various fissure openings and sizes.

2 Test materials and test methods

2.1 Test soil

The original loess selected for this test was taken from a project construction site in Xianyang city, Shaanxi province, with a brownish-yellow color and uniform soil quality, in which acicular pores are developed and the soil contains small amounts of calcareous streaks and calcareous binding. The sampling depth is the surface layer, which belongs to Late Pleistocene Q₃ loess. In the process of on-site soil sampling, chippers and shovels were used to chip out the original loess on the pit wall, and at the same time, the upper and lower surfaces of the soil samples were marked. After the soil samples were taken out, the original loess was immediately sealed with a plastic bag and adhesive tape in order to prevent the change in its initial water content, and the disturbance

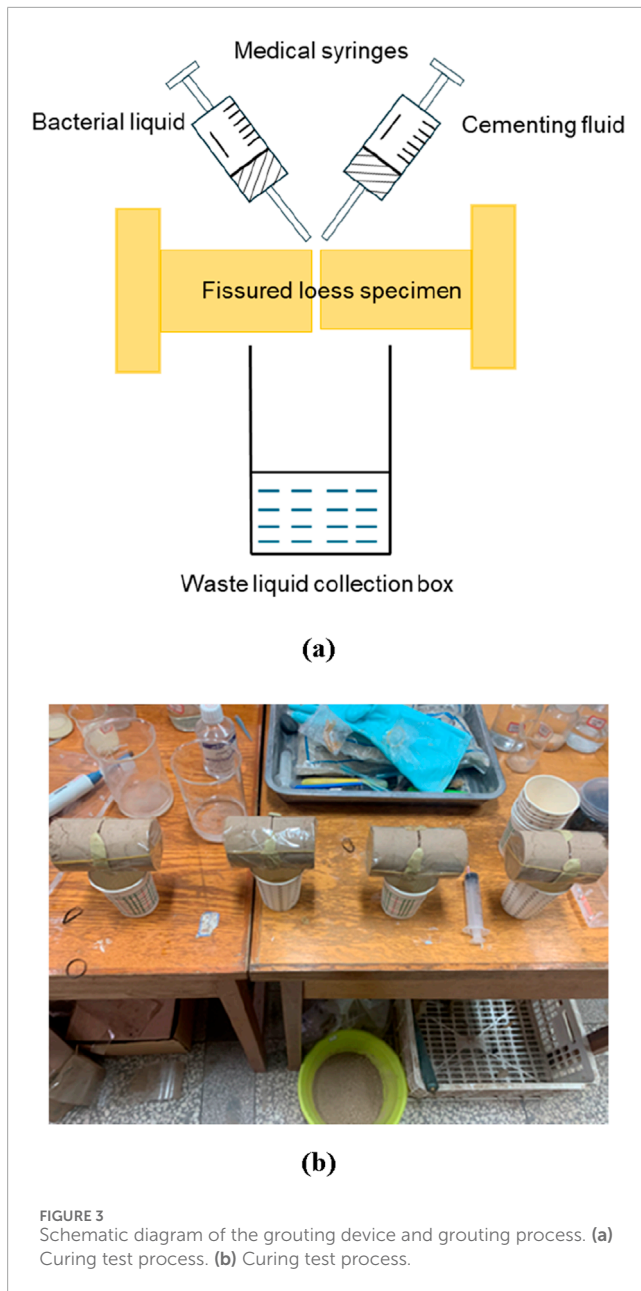
of the original loess was minimized during the transportation process; the photographs of on-site sampling are shown in Figure 1.

2.2 Bacterial solution and cementing solution

The microbial species used in this experiment is *Bacillus pasteurii*, which was purchased from the China Microbial Strain Conservation Center (strain number CGMCC1.3687). *Bacillus pasteurii* produces urease to hydrolyze urea and induce the generation of calcium carbonate in the MICP reaction, and at the same time, *Bartonella pasteurii* has strong environmental adaptability and produces a large amount of urease in the reaction, so it is often used for repair of fissures, reinforcement of sand bodies, and other applications.

When preparing the test bacteria solution, 100 mL of the culture solution should be prepared first, and, at the same time, a small amount of the NaOH solution should be added to adjust the pH of the culture solution to 9.0, and it should be sterilized in an autoclave for 30 min at 121°C. After sterilization, the liquid culture solution should be left to cool to room temperature. The activated *Pasteurella multocida* in the frozen tube should be inoculated into the liquid culture solution according to the ratio of the liquid culture solution to the bacterial solution of 100: 1. After the abovementioned operation, the mixed liquid culture solution was put into a constant temperature oscillation box, where the temperature of the oscillation box was set at 30°C and the rotation speed was 180 rpm, and culture was carried out for 16 h.

The cementing solution used in the experiment was a 1 mol/L CaCl₂ solution to provide calcium ions for the MICP reaction. The



composition of the liquid medium and culture solution components per 100 mL is shown in Table 1.

2.3 Test of CaCO_3 production in the MICP reaction catalyzed by urea

The MICP reaction process is composed of a series of complex biochemical reactions, mainly involving the urease enzyme produced by microorganisms to hydrolyze urea, forming carbonate, which then combines with calcium ions in the cementing solution to produce calcium carbonate precipitation. In this part of the test, there are two solutions to form a comparative test, and the control variable is the volume of the microbial solution and the cementing liquid added. In the process of the MICP reaction, urease produced during microbial metabolism interacts with calcium

ions and urea, which are abundant in the environment, thus forming calcium carbonate precipitation on the surface of soil particles or soil pores. At the same time, microorganisms also provide attachment points for CaCO_3 precipitation, which plays a role in cementing and filling the soil. The volumes of the microbial solution and cementing liquid are 5.8 mL and 10 mL, respectively. The mitigation ratio of the microbial solution to the gelling solution is 1:1.

2.4 Fissure-free loess curing test

Loess solidification adopts the step grouting method used by Liu et al. (2021), but biocement is underrepresented in the literature. After the curing test is completed, soil samples are removed and maintained. The microbiologically cured soil samples are then loaded into a strain-controlled triaxial instrument until the specimen fails, with the peak stress is recorded as the non-lateral compressive strength of the soil sample. First, the unconfined compressive strength test is carried out on the as-received soil samples, with a strength value of 173.95 kPa. The unconfined compressive strength of the cured soil samples is up to 863.8 kPa, and the strength of the treated soil samples was significantly improved compared to that of the untreated soil samples. The increase in the strength of microbial cured loess originates from the cementing and filling effects of calcium carbonate crystals, and the calcium carbonate deposits with cementing effects are more effective than calcium carbonate crystals in improving the strength of cured loess samples, which also verifies the feasibility of applying MICP in the reinforcement of fissured loess.

2.5 Scanning electron microscope test

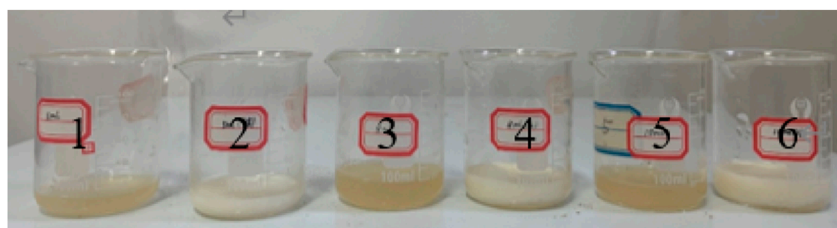
Scanning electron microscope tests are carried out on the loess before and after MICP curing, respectively, and the tests are photographed using a field emission scanning electron microscope, Gemini SEM 300. The sampling method is employed to cut the loess soil samples before and after MICP curing into $2\text{ cm} \times 1\text{ cm} \times 1\text{ cm}$ pieces, carve a 1 mm deep groove in the center, and then break them to obtain fresh sections after drying. The soil samples are subjected to electron microscope scanning at magnifications of 200, 500, 1,000, 2,000, and 4,000.

2.6 Fissure loess curing test

The test soil is air-dried in the natural environment, and then the air-dried loess is crushed with a soil grinder and passed through a 2 mm sieve. According to the test, the optimum moisture content of the specimen can be obtained as 16%, and the maximum dry density was 1.85 g/cm^3 . According to the optimum moisture content, the corresponding amounts of loess and pure water are measured and mixed thoroughly using a blender for 30 min. The soil–water mixture is then sealed in a plastic bag and left for 24 h to equilibrate the moisture. Finally, it is compacted in layers in a cylindrical steel mold with a diameter of 61.8 mm and a height of 125 mm. After the completion of sample making, the samples are



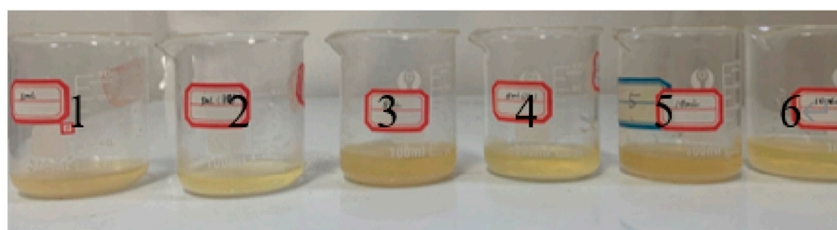
FIGURE 4
Appearance of the sample after grouting and curing.



(a)

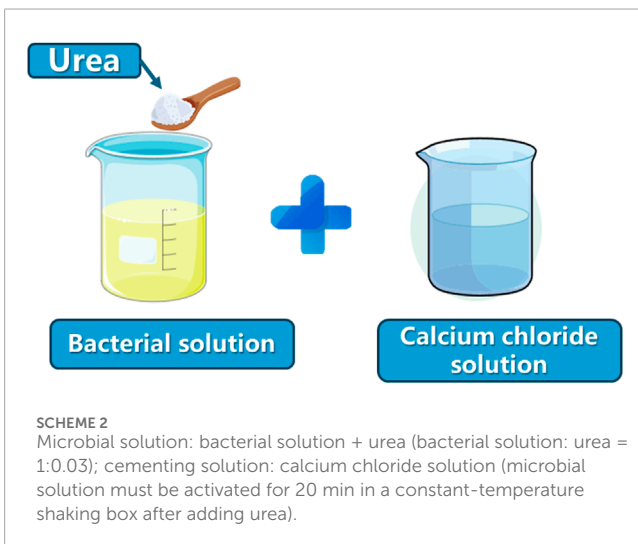
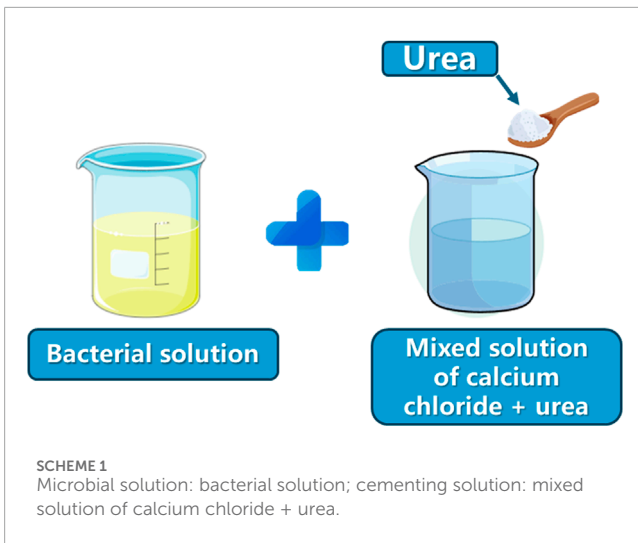


(b)



(c)

FIGURE 5
Process diagram of the MICP reaction catalyzed by urea. (a) MICP reaction for 1 minute. (b) MICP reaction for 30 minutes. (c) MICP reaction for 90 minutes.



cured in a standard constant temperature and humidity curing box at a room temperature of $20^{\circ}\text{C} \pm 2^{\circ}\text{C}$ and relative humidity at 95% for 7 days (Peng et al., 2024).

In order to make the fracture specimen closer to the natural state, a uniaxial tensile test was carried out on the specimen with a diameter of 61.8 mm and a height of 125 mm using the abovementioned prepared and maintained specimen. The specimen is pulled apart to obtain the fracture surface, which simulates a natural fracture surface, as shown in Figure 2.

The curing test of fissure loess is conducted by reinforcing the soil samples with step-by-step grouting. The test device includes a waste liquid collection box, a medical syringe, bacterial solution, cementing liquid, and biocement. Some of the biological cement is used to fix the fractured soil so that the injected solution flows along a specific route and does not spill out in other directions. The fissure openings of the test are controlled as 0.5, 1.0, and 1.5 mm; the test uses the biphasic grouting method to cure and fill the fissures, and the volume of the bacterial solution and cementing liquid injected each time is injected according to the optimal results of Test 2.3. In particular, urea at a concentration of 20 g/L is added to the bacterial

solution before the test, and then the solution is incubated in a shaking chamber for 30 min, with the speed of the shaking chamber set at 180 rpm. Using a medical syringe, the bacterial solution is first injected into the fissure at a uniform rate of 4 mL/min, and after standing for 2 h, the cementing solution is injected at the same rate, and a cycle is completed after standing for 6 h, with a total of 10 cycles conducted. The schematic diagram of the grouting device, the grouting process, and the appearance of the sample after grouting solidification are shown in Figure 3.

The direct shear test was conducted using a ring-cutter specimen, prepared with 10 mm above and below the centerline of the fissure interface, ensuring that the fissure in the fissured loess was located at the junction of the upper and lower shear boxes. In this test, the permeable stones in the upper and lower shear boxes were removed, allowing the specimen to shear more effectively along the solidified interfacial layer. This setup minimizes rupture and helps ensure the accuracy of the test results. The test was performed using a ZJ type strain-controlled direct shear instrument (quadruple), manufactured by the Nanjing Soil Instrument Factory. The fast shear method was adopted, with a shear rate set at $v = 0.8\text{--}1.2$ mm/min; the readings are recorded by taking pictures at intervals of 0.2 mm. The tests were carried out under normal loads of 100, 200, 300, and 400 kPa, and the cured specimens are generally sheared in 3–5 min. The appearance of the sample after grouting and curing is shown in Figure 4.

3 Results and discussion

3.1 Results of the urea-catalyzed CaCO_3 production test

The reaction process of MICP under the two schemes is shown in Figure 5; from the left to right, beakers 1, 3, and 5 correspond to Scheme 1; beakers 2, 4, and 6 correspond to Scheme 2. It can be observed from the figure that the MICP reaction is very rapid under the activation effect of urea. Figure 5a indicates that 1 min after the start of the MICP reaction following urea activation, the solution was filled with the generated calcium carbonate, indicating a rapid and intense reaction. Figure 5b shows that 30 min after the MICP reaction, white calcium carbonate began to appear in the non-urea-catalyzed solution, while at the same time, the calcium carbonate in the urea-catalyzed solution had begun to precipitate, indicating that the reaction was almost complete. Figure 5c shows that after 90 min of the MICP reaction, the MICP reaction under both scenarios had been completed, and the generated calcium carbonate had accumulated at the bottom of the beaker in the form of precipitation.

A comparison of calcium carbonate generation of different proportioning schemes is shown in Figure 6. It can be observed that the amount of calcium carbonate in Scheme 2 was increased by more than 20% compared with that in Scheme 1. In addition, as the injected volume increased, the rate of calcium carbonate generation showed a trend of initially increasing and then decreasing. The highest improvement rate reached approximately 30% when both the microbial solution and cementing solution were 8 ml. At the same time, the reaction time after catalyzing was shortened by approximately fourfold, requiring only 30 min for complete precipitation. Therefore, adding a certain volume of urea to the bacterial solution can first

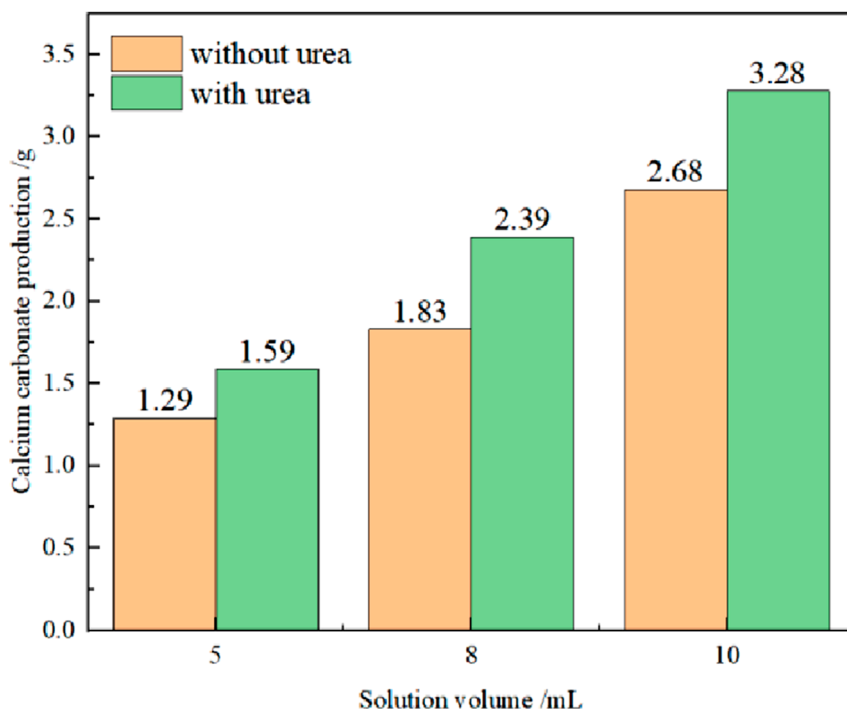


FIGURE 6 Comparison chart of calcium carbonate production.

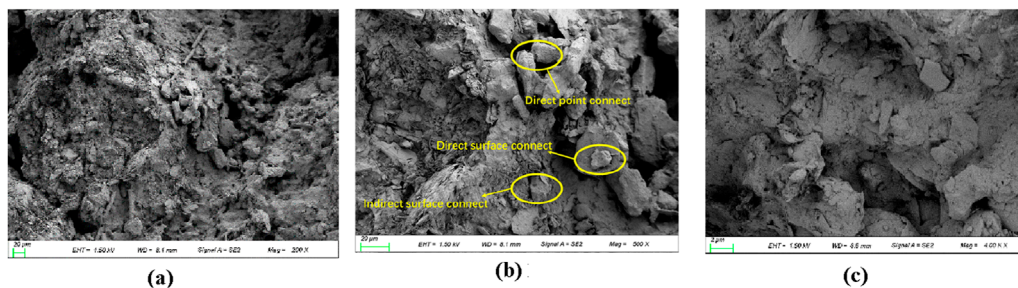


FIGURE 7 Microstructure of loess before MICP curing. (a) Loess structure before solidification under 200 x. (b) Loess structure before solidification under 500 x. (c) Loess structure before solidification under 4,000 x.

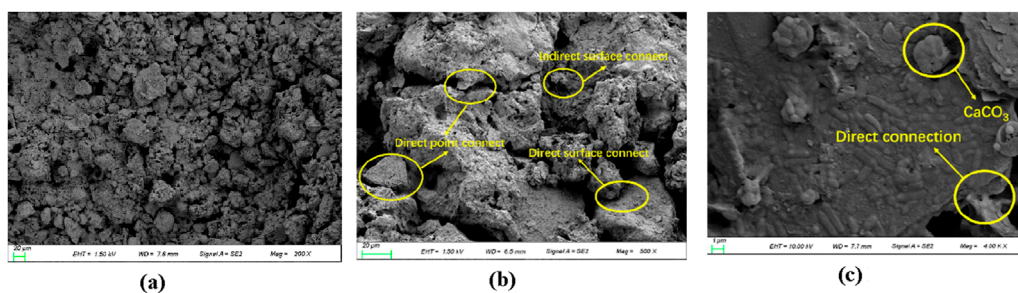
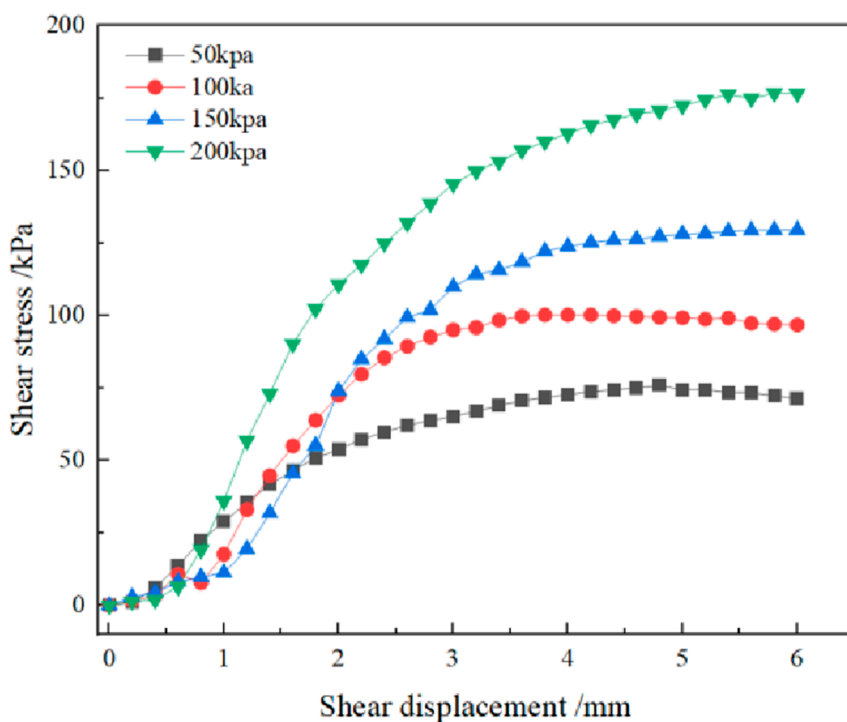
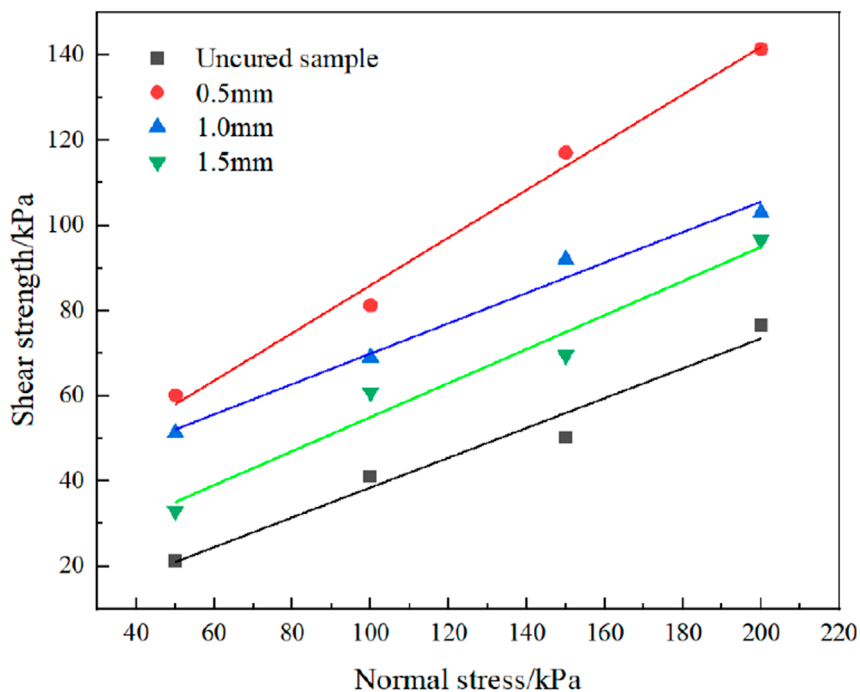


FIGURE 8 Microstructure of loess after MICP curing. (a) Loess structure after solidification under 200 x. (b) Loess structure after solidification under 500 x. (c) Loess structure after solidification under 4,000 x.



(a)



(b)

FIGURE 9 Correlation curve of a direct shear test. **(a)** Relationship curve between shear stress and shear displacement of a 1.0 mm crack opening. **(b)** Relationship curve between shear strength and normal stress at different crack openings.

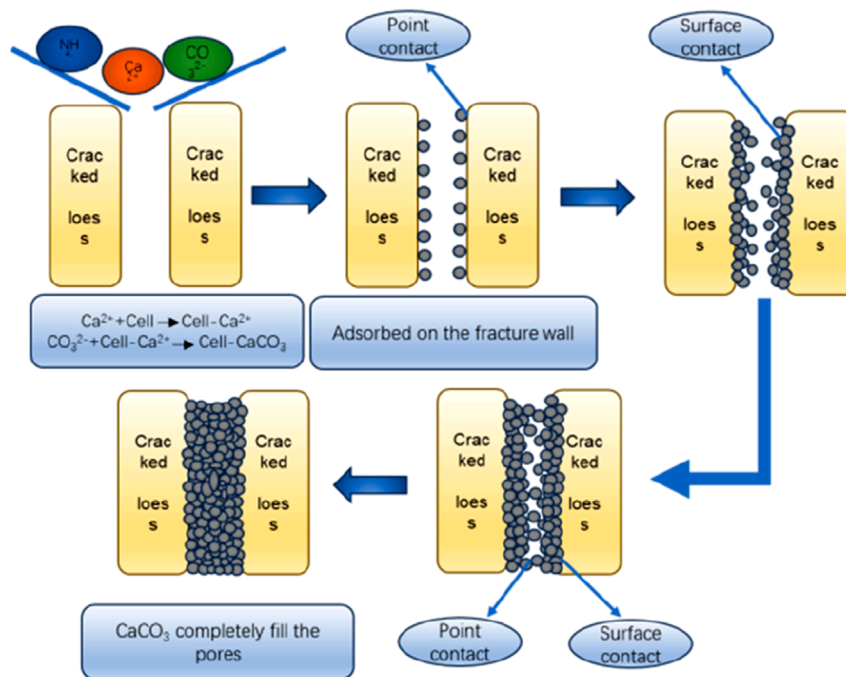


FIGURE 10
Microscopic mechanism diagram of MICP curing fractured loess.

promote cell production, greatly increasing the activity of the bacterial solution. This accelerates the MICP reaction process, increases the CaCO_3 production rate (Zhu et al., 2025), and greatly improves the cementing ability of the MICP reaction.

3.2 Comparative analysis of microscopic results of loess before and after MICP treatment

Figures 7, 8 show the SEM images of loess before and after MICP curing, and it was observed that a large number of rod-like substances were adsorbed on the surface of soil particles, which resembled the size and shape of the microorganisms observed under the microscope, with a length of approximately $2\text{--}5\ \mu\text{m}$ and a diameter of approximately $0.5\ \mu\text{m}$, which were identified as *Bacillus bacillus*. Compared with untreated loess, calcium carbonate crystals were generated on the surface of soil particles after MICP treatment, and some CaCO_3 was deposited in the pores between soil particles, filling them; some were adsorbed and connected between two soil particles, cementing them together; some covered the surface of soil particles, increase their roughness, and it was observed that the bacteria tended to pile up and grow in areas with smaller pores.

The characteristics of the cured loess are as follows: the surface contact between the agglomerates increases significantly. This is because the calcium carbonate generated by the MICP reaction can act as the cementing material between the agglomerates, and the generated calcium carbonate is adsorbed around the point contact between the agglomerates, causing the point contact to evolve into surface contact. The pore area of the loess becomes smaller, the surface of each agglomerate is adsorbed and wrapped with a lot of

cemented film, and the particle morphology tends to be smoother than that of the original loess; the intra-granular microporosity is relatively reduced because the calcium carbonate precipitation generated by microorganisms can act as a filler and cementing agent for the intra-granular microporosity.

After the observation and analysis of the SEM images of loess after MICP curing, it was found that MICP acts as a binder to adhere loess particles and has a limited effect on the filling of the overhead pores. The reason is that the diameter of *Bacillus pasteurii* is generally $2\text{--}5\ \mu\text{m}$, and the caliber of the overhead pores is larger, indicating that the bacteria are inclined to be adsorbed on the surface of the soil particles and both sides of the contact points of the particles. When the cementing solution is added dropwise, the calcium carbonate precipitation formed can play an effective role in cementing the loess, increasing its adhesion and contributing to the curing of the loess. The distribution of calcium carbonate deposition depends on the distribution of different pores in loess; the distribution of shelf, mosaic, and cement pores in loess is not uniform and regular, so the calcium carbonate deposition is also characterized by random distribution and is not uniformly distributed all over the loess cut surface. Among them, in the mosaic and cement pores, calcium carbonate plays a cementing role. Calcium carbonate provides “strong cementation” because it increases the loess particles between the mutual bite and contact area, which is conducive to their stability. The filling calcium carbonate plays a role of “weak cementation,” and in the presence of water or pressure, it is prone to falling into larger pores. However, the filling calcium carbonate also increases the soil density, which, to a certain extent, contributes to soil stabilization. Moreover, the calcium carbonate crystals that play a role in filling will be stacked up and become larger with an increase in the number injections of bacterial and cementing liquids, eventually causing neighboring soil particles to become cemented together.



(a)



(b)

FIGURE 11
Single-crack loess sample after solidification. **(a)** Solidified fractured loess sample 1. **(b)** Solidified fractured loess sample 2.

TABLE 2 Comparison table of loess curing methods with different sizes of crack openings.

	Direct shear specimen	Cracked loess sample 1	Cracked loess sample 1
Crack opening	1.0 mm	1.0 mm	1.5 mm
Fracture cross-sectional area	2,999.62 mm ²	8,500 mm ²	22,500 mm ²
Grouting method	Two-phase grouting	Two-phase grouting	Two-phase grouting
Cementing round	10	17	30
Microbial solution dosage	160 mL	272 mL	480 mL
Maintenance days	0	0	3
Interstitial filling material	---	---	Quartzite

3.3 Straight shear test results

The binding strength of samples was measured by a straight shear test. Taking 1.0 mm fissure openings as an example, the relationship curves between shear stress and shear displacement of fissure loess specimens under four levels of normal stresses, namely, 100 kPa, 200 kPa, 300 kPa, and 400 kPa, are shown in [Figure 9a](#) after curing and grouting with the MICP reaction. According to the relationship curve, the shear process of cured fissured loess can be divided into three stages: the first process is the compression stage, in which the slope of the curve gradually increases from the origin of the coordinate axis; the second process is the elasticity stage, in which the shear stress increases with the rate of shear displacement, and the slope of the curve is steeper; the third process is the yielding stage, in which the slope of the curve gradually decreases, and the specimen is sheared.

As shown in [Figure 9b](#), as the size of the specimen fissure opening increases, the cohesion at the specimen fissure interface significantly decreases. This is because as the fissure opening becomes larger, the tension of the grouting liquid at the fissure becomes smaller; the bacterial liquid easily flows out along the structural surface; the bacteria are not easily fixed on the structural surface, and there are fewer nucleation sites when the cementing liquid is infused, resulting in poor grout curing; under the condition that the structural surfaces of the fissure specimens are the same, the internal friction angle of the fissure opening of 1.0 mm is slightly reduced than that of the fissure opening of 0.5 mm, but the difference is not significant. In contrast, when the fissure opening is 1.5 mm, the internal friction angle at the 1.5 mm fissure opening significantly decreases compared to the internal friction angles at the 0.5 mm and 1.0 mm openings. This is due to the large fissure opening, which causes poor occlusion between the concave and convex structures of the soil surface, and as a result, the internal friction angle is mainly supported by the calcium carbonate cement, leading to a

significant decrease in the internal friction angle at the 1.5 mm fissure opening decreases significantly compared to that at 0.5 mm and 1.0 mm openings.

According to the abovementioned microscopic scanning electron microscope test results, it can be observed that the MICP method of curing loess mainly involves changing the contact mode between calcium carbonate crystals and the loess body to achieve curing. When MICP cures fissure loess, the calcium carbonate generated by MICP first adheres to the two sides of the fissure, forming point contact, and with increasing point contact, it gradually evolves into surface contact. With an increase in the amount of calcium carbonate generated, the fissure is gradually filled from the two sides toward the center, eventually leading to point contact in the middle. At this point, the MICP solution is continued to be injected until the point contact in the middle evolves into a surface contact; the fissure is then gradually filled, completing the curing of fissure loess ([Peng et al., 2023](#)). The micro-mechanism of cured fissure loess is shown in [Figure 10](#).

3.4 Curing test of large-sized fissure loess

According to the abovementioned test results proving that MICP can effectively repair small-sized fissures, next, this paper studied MICP repairing of large-sized fissures. Due to the difficulty of collecting loess samples with natural fissures, this test adopts the manual method to split the retrieved original loess to obtain the fissured loess samples with a single fissure. In this test, a total of two pieces of primary loess are split. The first piece of primary loess specimen size is 100 mm × 85 mm × 80 mm, which is recorded as specimen 1; the second piece of primary loess is 150 mm × 150 mm × 100 mm, which is recorded as specimen 2.

After aligning the two flaps of the single-fissure original loess specimen with a frame, the fissure size of specimen 1 is controlled at 1.0 mm and that of specimen 2 is controlled at 1.5 mm using different sizes of plugging rulers; because of the larger fissure openings and areas in the reinforced soil samples of specimen 2, standard quartz sand was filled in the fissures in order to increase the effectiveness of its reinforcement. Specimen 2 is tested before the test, and the sand-filling method is used to measure the volume of the fissure by filling the fissure with airborne sand. After the test, the volume of the fissure of specimen 2 is 21.73 cm³ at the 1.5 mm opening. Due to its large fissure opening, specimen 2 is cured via the sand addition method, i.e., filling the fissure with quartz sand every 3 days.

As shown in [Figure 11](#), it can be observed that the two specimens are well-bonded, indicating that MICP has a strong cementing ability; even in the case of larger size or larger fissure openings, it can still have a very good curing effect.

3.5 Effect of the MICP solution on the curing of fissure loess of different sizes

The number of cementation rounds, microbial solution dosage, and other aspects of small- and large-sized fissure loess are compared to analyze the effect of size on the curing effect of fissure loess, as shown in [Table 2](#):

Table 2 reveals that under the same fissure opening, the fissured loess body can still be effectively cemented by increasing the number of cementing rounds and the amount of the microbial solution. Therefore, it is proved that the effect of cementation can be achieved by increasing the dosage of the MICP solution for specimens of different sizes under the same fissure opening.

4 Conclusion

The MICP curing test of crack-free loess is carried out, and the microstructure of samples before and after curing is observed by SEM, which reveals the microscopic mechanism of MICP curing in loess, evaluating the MICP reaction efficiency of the microbial solution under the catalysis of urea or not and obtaining the optimal grouting scheme of microbial solution. The curing test is carried out on samples with crack openings of different sizes, and the influence law of crack opening on the curing effect is obtained through the shear test. The main conclusions are as follows:

- (1) The strength of the loess significantly improves in the MICP curing test, and the SEM test shows that the calcium carbonate produced by the MICP reaction can be used as a cementing substance between aggregates, and the generated calcium carbonate is adsorbed around the point contact between aggregates, which makes the point contact evolve into surface contact.
- (2) The experiment of CaCO_3 production in the MICP reaction under the catalysis of urea revealed that when the microbial and cementing solutions are mixed in amounts of 8 mL, the CaCO_3 production increases by approximately 30%, and at the same time, the reaction efficiency improves after urea catalysis, the time was shortened by four times compared with that without catalysis, and the reaction can be completed in 30 min.
- (3) Through the curing test of fractured loess, it is found that MICP can effectively cure fractured loess when the crack opening is less than 1.0 mm, and the direct shear test revealed that the maximum cohesion after curing can reach 38.18 kPa and the internal friction angle can reach 33.42° . After solidification, the strength of the soil on both sides of the fractured loess structural plane increases, and the internal friction angle increases. With an increase in the size of the crack opening, the cohesion at the crack interface decreases significantly, resulting in a poor grouting curing effect.

References

- Ahmad, I., and Chandra, R. (2019). Micromorphological study of kashmir loess-paleosol sediments: a tool for stratigraphic and paleoclimatic reconstruction. *Earth Sci. India* 12 (2). doi:10.1016/j.conbuildmat.2023.133810
- Chen, M. Y., Chen, R. P., Chen, Y. Q., Kang, X., et al. (2023). Chloride ion transport in unsaturated ultra-high performance concrete cracks under high hydraulic pressures. *Constr. Build. Mater.* 409 (15), 133810. doi:10.1016/j.conbuildmat.2023.133810
- Chen, Y. Q., Wang, S. Q., Tong, X. Y., Kang, X., et al. (2022). Crystal transformation and self-assembly theory of microbially induced calcium carbonate precipitation. *Appl. Microbiol. & Biotechnol.* 106, 3555–3569. doi:10.1007/s00253-022-11938-7
- Cintia F., Y., Pereira, E. I., Mattoso, L. H. C., Matsunaka, T., and Ribeiro, C. (2016). Slow release fertilizers based on urea/urea-formaldehyde polymer nanocomposites. *Chem. Eng. J.* 287 (287), 390–397. doi:10.1016/j.cej.2015.11.023
- Clifford, Y. T. A. I., Mengchun, C., Rongjiong, S., and Chen, T. G. (2008). Magnetic effects on crystal growth rate of calcite in a constant-composition environment. *J. Cryst. Growth* 310 (15), 3690–3697. doi:10.1016/j.jcrysgro.2008.05.024
- Gao, Y., Zhang, F., Lei, G., and Li, D. (2013). An extended limit analysis of three-dimensional slope stability. *Géotechnique*, 63(6): 518–524. doi:10.1680/geot.12.t.004
- Gu, K., and Chen, B. (2020). Loess stabilization using cement, waste phosphogypsum, fly ash and quicklime for self-compacting rammed earth construction. *Constr. Build. Mater.* 231, 117195. doi:10.1016/j.conbuildmat.2019.117195
- Guimaraes, G. F., Mulvaney, R. L., Khan, S. A., Cantarutti, R. B., and Silva, A. M. (2016). Comparison of urease inhibitor N(n-butyl)thiophosphoric triamide and oxidized charcoal for conserving urea-N in soil. *J. Plant Nutr. Soil Sci.* 179 (4), 520–528. doi:10.1002/jpln.201500622

Data availability statement

The raw data supporting the conclusions of this article will be made available by the authors, without undue reservation.

Author contributions

CP: methodology and writing – original draft. CZ: data curation, funding acquisition, validation, and writing – review and editing. TJ: writing – review and editing.

Funding

The author(s) declare that financial support was received for the research and/or publication of this article. This manuscript was supported by the Nanjing Hydraulic Research Institute under grant nos BK20221193 and Y323008 and the Xinjiang Shui Fa Water Group under grant no. JWYX36/2022.

Conflict of interest

The authors declare that the research was conducted in the absence of any commercial or financial relationships that could be construed as a potential conflict of interest.

Generative AI statement

The author(s) declare that no Generative AI was used in the creation of this manuscript.

Publisher's note

All claims expressed in this article are solely those of the authors and do not necessarily represent those of their affiliated organizations, or those of the publisher, the editors and the reviewers. Any product that may be evaluated in this article, or claim that may be made by its manufacturer, is not guaranteed or endorsed by the publisher.

- He, J., Chu, J., Liu, H. L., Gao, Y. F., and Li, B. (2016). Research progress of microbial geotechnical technology. *J. Geotechnical Eng.* 38 (04), 643–653.
- He, S. L., Wang, W., Huang, D. K., and Liu, Z. Y. (2008). Study on crystallization kinetics of CaCO₃ in NaCl salt solution by using calcium ion selective electrode. *Salt Industry Chem. Industry* (5), 7–11.
- Jia, Y. M., Hu, Z. Y., Mu, J., Zhang, W., Xie, Z., and Wang, G. (2020). Preparation of biochar as a coating material for biochar-coated urea. *Sci. Total Environ.* 731, 139063. doi:10.1016/j.scitotenv.2020.139063
- Jiang, M., Zhang, F., Hu, H., Cui, Y., and Peng, J. (2014). Structural characterization of natural loess and remolded loess under triaxial tests. *Eng. Geol.* 181, 249–260. doi:10.1016/j.enggeo.2014.07.021
- Li, G. Y., Wang, F., Ma, W. R., Fortier, R., Mu, Y., Mao, Y., et al. (2018). Variations in strength and deformation of compacted loess exposed to wetting-drying and freeze-thaw cycles. *Cold Region Sci. Technol.* 151, 159–167. doi:10.1016/j.coldregions.2018.03.021
- Li, J., Hou, Q. M., Zhang, X. Q., and Zhang, X. B. (2025). Microbial-induced mineral carbonation: a promising approach for improving Carbon sequestration and performance of steel slag for its engineering utilization. *Dev. Built Environ.* 21, 100615. doi:10.1016/j.dibe.2025.100615
- Li, P., Xie, W., Pak, R. Y. S., and Vanapalli, S. K. (2019). Microstructural evolution of loess soils from the Loess Plateau of China. *Catena* 173, 276–288. doi:10.1016/j.catena.2018.10.006
- Liu, H., Hu, P. F., Wang, S. H., Liu, N. F., Hu, W. L., Gu, H. Q., et al. (2022). Experimental study on the influence of acid solution on the tensile strength of undisturbed loess. *J. Civ. Environ. Eng.* 44 (5), 109–117. doi:10.11835/j.issn.2096-6717.2021.009
- Liu, X. J., Fan, J. Y., Yu, J., and Gao, X. (2021). Solidification of loess using microbial induced carbonate precipitation. *J. Mt. Sci.* 18 (01), 265–274. doi:10.1007/s11629-020-6154-8
- Liu, Z., Liu, F., Ma, F., Wang, M., Bai, X., Zheng, Y., et al. (2015). Collapsibility, composition, and microstructure of loess in China. *Can. Geotechnical J.* 53 (4), 673–686. doi:10.1139/cgj-2015-0285
- Luo, M., and Lu, Z. (2000). Kinetic study on crystallization process of calcium carbonate. *Fine Chem. Ind.* (8), 463–466.
- Morris, P. H., and Williams, D. J. (1992). Cracking in drying soils. *Can. Geotechnical J.* 29, 263–277.
- Muñoz-Castelblanco, J. A., Pereira, J. M., Delage, P., and Cui, Y. (2012). The water retention properties of a natural unsaturated loess from northern France. *Geotechnique* 62 (2), 95–106. doi:10.1680/geot.9.p.084
- Peng, C., Xie, J. C., Ouyang, Y., Li, C., and Wu, D. B. (2024). Effect test and mechanism analysis of EICP in repairing precast micro-cracks in concrete. *J. South China Univ. Nat. Sci. Ed.* 38 (04), 56–64. doi:10.19431/j.cnki.1673-0062.2024.04.007
- Peng, L. Y., Du, X. T., Qi, J. L., and Zhu, T. Y. (2023). Study on permeability characteristics and micro-mechanism of silty soil reinforced by MICP. *J. Beijing Jiaot. Univ.* 47 (06), 154–162.
- Shao, X., Zhang, H., and Tan, Y. (2018). Collapse behavior and microstructural alteration of remolded loess under graded wetting tests. *Eng. Geol.* 233, 11–22. doi:10.1016/j.enggeo.2017.11.025
- Spencer, E. (1967). A method of analysis of the stability of embankments assuming parallel inter-slice forces. *Géotechnique* 17 (1), 11–26. doi:10.1680/geot.1967.17.1.11
- Sun, P., Peng, J. B., Chen, L., Lu, Q., and Igwe, O. (2016). An experimental study of the mechanical characteristics of fractured loess in western China. *Bull. Eng. Geol. Environ.* 75 (4), 1639–1647. doi:10.1007/s10064-015-0793-y
- Utili, S. (2013). Investigation by limit analysis on the stability of slopes with cracks. *Géotechnique* 63 (2), 140–154. doi:10.1680/geot.11.p.068
- Wei, T., Fan, W., Yu, N., and Wei, Y. n. (2019). Three-dimensional microstructure characterization of loess based on a serial sectioning technique. *Eng. Geol.* 261, 105265. doi:10.1016/j.enggeo.2019.105265
- Wen, B. P., and Yan, Y. J. (2014). Influence of structure on shear characteristics of the unsaturated loess in Lanzhou, China. *Eng. Geol.* 168, 46–58. doi:10.1016/j.enggeo.2013.10.023
- Xiao, X. M., Yu, L., Xie, F. W., Bao, X., Liu, H., Ji, Z., et al. (2017). One-step method to prepare starch-based superabsorbent polymer for slow release of fertilizer. *Chem. Eng. J.* 309 (309), 607–616. doi:10.1016/j.cej.2016.10.101
- Yan, C. G., Liang, Z. R., Jia, Z. L., Lan, H. X., Shi, Y. L., Yang, Y. L., et al. (2023). Review on surface protection technologies of loess slope. *J. Traffic Transp. Eng.* 23 (4), 1–22. doi:10.19818/j.cnki.1671-1637.2023.04.001
- Zhou, J. (2019). *Experimental study on small crack simulation and grouting process in rammed earthen sites[D]*. Lanzhou: Lanzhou University. (in Chinese).
- Zhu, R., Xing, W., Guo, W. L., Huang, Y. H., Zhou, F., Wang, X. D., et al. (2025). Study on freeze-thaw characteristics and micro-mechanism of silt reinforced by microorganisms. *J. Geotechnical Eng.* 47 (02), 376–387.